cogent
engineering

CrossMark

SYSTEMS & CONTROL | RESEARCH ARTICLE

Stochastic stability for a model representing the intake manifold pressure of an automotive engine

Alessandro N. Vargas[1]*, Leonardo Acho[2], Edison Bonifacio[3], Walter Arens[4] and João B.R. do Val[4]

Abstract: The paper presents conditions to assure stochastic stability for a nonlinear model. The proposed model is used to represent the input-output dynamics of the angle of aperture of the throttle valve (input) and the manifold absolute pressure (output) in an automotive spark-ignition engine. The automotive model is second moment stable, as stated by the theoretical result—data collected from real-time experiments supports this finding.

Subjects: Dynamical Systems; Electrical & Electronic Engineering; Stochastic Models & Processes

Keywords: Stochastic systems; stability; automotive models; combustion engines

1. Introduction

In combustion engines, the correct adjustment of the air-fuel (A/F) ratio of the gas mixture used into the combustion chamber is of foremost importance (Guzzella & Onder, 2010, Sec. 2.7; Stotsky, 2009, Sec. 2.3). The ratio chosen for the mixture must be set to the stoichiometric ratio of the corresponding fuel as it influences, for instance, the efficiency of the engine's catalytic converter and sets the level of emission pollutants, see the monograph (Heywood, 1988) for further details.

Adjustment of the A/F ratio is done in closed loop mode via an oxygen sensor installed at the exhaust duct. For a given air mass, the controller calculates the fuel amount based on stoichiometry (Guzzella & Onder, 2010, Sec. 4.3). Thus the A/F ratio depends primarily on the air mass flow in the intake manifold, see the diagram in Figure 1. The air entering into the intake manifold crosses the

ABOUT THE AUTHORS

Alessandro N. Vargas received the PhD degree in Electrical Engineering from the School of Electrical and Computer Engineering of the University of Campinas, Brazil, in 2009. Since 2007, he has held a position of Control Systems professor at the Universidade Tecnologica Federal do Parana, Brazil. His research interests include stochastic systems and control with applications in electronics and electrical engineering. The research presented in this paper was developed in Lab Control [www.labcontrol.xyz], a research laboratory located at Universidade Tecnològica Federal do Paranà (UTFPR), Brazil. Lab Control is dedicated to develop research on Control Systems and Automation. The research received finantial support from the Brazilian agency CAPES under grant CAPES 88881.030423/2013-01, Sistemas estocàsticos com aplicações em engenharia automotiva [Programa Pesquisador Visitante Especial - PVE].

PUBLIC INTEREST STATEMENT

The paper presents a nonlinear model for representing the relation between the angle of aperture of the throttle valve (input) and the manifold absolute pressure (output) in *spark-ignition engines*. Besides, the paper shows that the model is stable provided that some mild conditions are satisfied. Experimental data support the main findings.

cogent ·· oa

cogent·engineering

Figure 1. Diagram of the cylinder block and air flow connections in a typical combustion engine.
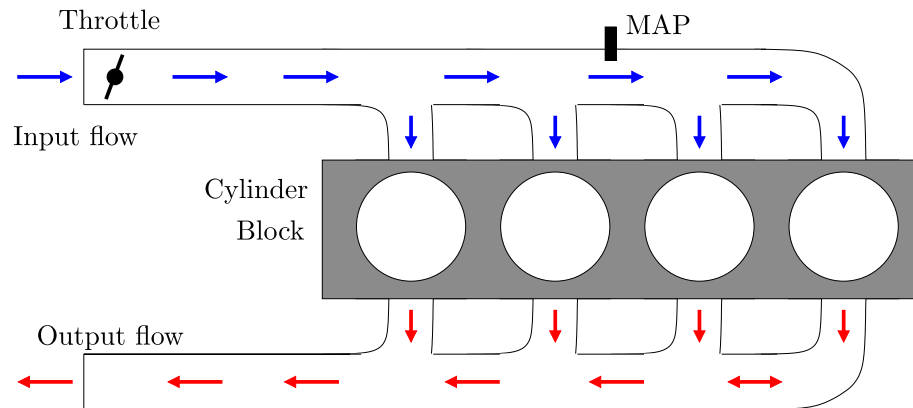
throttle, a device with a circular plate that is used to adjust the mass air flow. The air flows into the intake manifold and then through the cylinder intake runners where the fuel injectors are installed. The up and down movement of the pistons creates a vacuum in the intake manifold and the A/F mixture flows into the cylinders. This vacuum can be measured through a sensor called Manifold Absolute Pressure (MAP). The pressure value indicated by the MAP sensor is of key importance, since one can easily calculate the mass air flow through the well-known speed-density Equation (Guzzella & Onder, 2010, Ch. 2; Stotsky, 2009, Equation (2.1), p. 16). This paper contributes towards this problem by presenting a stochastic nonlinear model that aims to characterize the input-output relation between the angle of aperture of the throttle device and the MAP value, as detailed in the sequence.

The literature is rich for models that aim to characterize the dynamics of spark-ignition combustion engines. Nowadays the most accepted model comes from the seminal work (Hendricks & Sorenson, 1990), which was the first to coin the term *mean value engine model* (MVEM). Although suffering from a certain level of empiricism (Hendricks, 1997, p. 389), the MVEM model is quite complete and general for modeling the three main spark-ignition engine subsystems, i.e. intake manifold, crank shaft, and fuel supply subsystems (Balluchi, Benvenuti, Di Benedetto, Pinello, & Sangiovanni-Vincentelli, 2000; Casavola, Famularo, & Gagliardi, 2013; Guzzella & Onder, 2010, Ch. 2; Hendricks, 1997; Hendricks & Sorenson, 1990; Tang, Weng, Dong, & Yan, 2009). But this general model imposes a drawback for the analysis of any subsystem in particular because it requires all subsystems working together in a strongly nonlinear, coupled fashion. Consequently determining the specific throttle-MAP relation through the MVEM model requires the knowledge of all subsystems, which is a difficult task–identifying the MVEM model requires simultaneous measurements of many sensors (Fleming, 2001) and can be time-consuming (Hendricks, 1997, p. 391). An advantage of our approach is that it aims to simplify this task, i.e. the throttle-MAP relation is studied here in the viewpoint of a unique single-input single-output relation, and for this reason our approach is completely detached from the ones in the literature. Finding a model for the throttle-MAP relation represents the main practical contribution of this paper.

Indeed, our main practical contribution is to propose a stochastic nonlinear model for the throttle-MAP relation. To account this relation, we adopt a structure borrowed from the nonlinear ARX model (Ljung, 1999, Ch. 5; Pearson, 2003; Sjöberg et al., 1995), as follows. Let y_k be a real-valued variable representing the output, measured by an appropriate device attached to the system, corresponding to the input values $(u_0, u_1, \ldots, u_k)$ applied in the system until the *k*-th stage. If we let

$$Y_k = (y_k, \ldots, y_{k-d}, u_k, \ldots, u_{k-d}), \quad \forall k \geq d, \tag{1}$$

for some integer $d \geq 0$, then the identification problem consists of finding a function $f(\cdot)$ such that

$$y_{k+1} = f(Y_k, W_k), \quad \forall k \geq d,$$

(2)

where $\{W_k\}$ represents some finite-dimensional stochastic process.

The exact format of the function $f(\cdot)$ is usually unknown. As a first attempt, one may resort to linear maps (Ortner & del Re, 2007). Nonlinear maps, though, expand the throttle-MAP representation—one may check whether the real-time measured data resembles the simulated one produced by some benchmark some nonlinear functions (Ljung, 1999, Ch. 5; Sjöberg et al., 1995). This strategy is accounted in our study, as detailed next.

From the theoretical point of view, the main contribution of this paper is to present a sufficient condition to the second moment stability of the stochastic nonlinear system in (2), under some assumptions on $f(\cdot)$.

For sake of completeness, let us recall the definition of such stability concept (see also Li, Sui, Tong, 2016; Wu, Cui, Shi, & Karimi, 2013; Yin, Khoo, Man, & Yu, 2011; Zhao, Feng, Kang, 2012 for further details).

Definition 1.1 Arnold (1974, p. 188), Vargas and do Val (2010) We say the nonlinear stochastic system in (2) is second moment stable if there exists a constant $c > 0$ (which may depend on the initial values $(y_0, \dots, y_d)$) such that

$$\mathsf{E}\left[y_k^2\right] \leq c, \quad \forall k > d,$$

where $\mathsf{E}[\cdot]$ represents the expected value operator.

A conclusion drawn from our findings is that the identified throttle-MAP stochastic model, obtained from real-time experiments and written as in (2), is second moment stable. This fact sets the practical benefit of this paper.

The paper is organized as follows. Section 2 quotes the notation, definitions, and presents the stability result. Section 3 presents the experiments that were carried out to obtain a stochastic model for the throttle-MAP nonlinear relation. Finally, Section 4 presents some concluding remarks.

2. Basic definitions and main result

Let us denote the *n*-dimensional Euclidean space by $\mathbb{R}^n$ and the corresponding norm by $\|\cdot\|$; the set made up by matrices of dimension $n \times m$ is denoted by $\mathbb{R}^{n \times m}$. An element x from $\mathbb{R}^n$ is denoted by $x = \left[x_{[1]} \dots x_{[n]}\right]'$. Given a matrix $V = [v_1 | \cdots | v_m] \in \mathbb{R}^{n \times m}$, the notation $\mathsf{vec}(V)$ denotes the vectorization of the matrix V, i.e.

$$\mathsf{vec}(V) = \begin{bmatrix} v_1 \\ \vdots \\ v_m \end{bmatrix} \in \mathbb{R}^{nm}.$$

Denoting the symbol $\otimes$ by the Kronecker product, we recall that $(N' \otimes M)\,\mathsf{vec}(V) = \mathsf{vec}(MVN)$, where M, N, and V are matrices of compatible dimensions (Brewer, 1978).

Hereafter, we assume that the system in (2) is governed by $(\Omega, \mathcal{F}, \{\mathcal{F}_k\}, P)$, a fixed filtered probability space, and that the input sequence $\{u_k\}$ takes values in $\mathbb{R}$. In addition, we assume that $\{W_k\}$ on $\mathbb{R}^\ell$ represents an independent and identically distributed (i.i.d.) stochastic process with null mean and covariance matrix identical to the identify.

The authors of (Sjöberg et al. 1995, Sec. 4.1) suggest the use of both sigmoid and Gaussian bell functions as candidates for representing the nonlinear term in (2). This idea motivated us to sum these two functions in order to obtain the function $g{:}\mathbb{R}^s \mapsto \mathbb{R}$ as

$$g(x) = \mu + \sum_{i=1}^{n} \left(a_i \left(\exp\left(\alpha_i x - c_i \right) + 1 \right)^{-1} + b_i \exp\left(-\left(\beta_i x - d_i \right)^2 / \left(2e_i^2 \right) \right) \right), \quad \mu \neq 0, \quad \forall x \in \mathbb{R}^s, \tag{3}$$

where α_i and β_i are s-dimensional constant row vectors; a_i, b_i, c_i, d_i, e_i are real-valued constants; and n is some finite integer.

Remark 1   It follows from the definition of g in (3) that

$$|g(x)| \leq |\mu| + \sum_{i=1}^{n} |a_i| + |b_i|, \quad \forall x \in \mathbb{R}^s.$$

Thus the function g in (3) is bounded.

Setting some row vectors $H_i \in \mathbb{R}^{1 \times s}$, $i = 1, \dots, \ell$, and $A \in \mathbb{R}^{1 \times s}$, we can define the function $f{:}\mathbb{R}^s \times \mathbb{R}^\ell \mapsto \mathbb{R}$ as in (2) as follows:

$$f(x, w) = \left(A + \sum_{i=1}^{\ell} H_i w_{[i]} \right) x + g(x), \quad \forall x \in \mathbb{R}^s, \; w \in \mathbb{R}^\ell. \tag{4}$$

With f as in (4), the nonlinear stochastic system (2) now reads at the k-th stage as

$$y_{k+1} = f(Y_k, W_k) \quad \text{subject to (1)}. \tag{5}$$

Before presenting the main theoretical contribution of this paper, let us introduce some additional notation. Consider the matrices

$$\mathcal{A} = \begin{bmatrix} 0 & 1 & 0 & \cdots & 0 \\ 0 & 0 & 1 & \cdots & 0 \\ \vdots & \vdots & \vdots & \ddots & \vdots \\ 0 & 0 & 0 & \cdots & 1 \\ A_{[d+1]} & A_{[d]} & A_{[d-1]} & \cdots & A_{[1]} \end{bmatrix}, \quad \mathcal{H}_i = \begin{bmatrix} 0 & 0 & \cdots & 0 \\ \vdots & \vdots & \ddots & \vdots \\ 0 & 0 & \cdots & 0 \\ H_{[d+1],i} & H_{[d],i} & \cdots & H_{[1],i} \end{bmatrix}, \quad i = 1, \dots, \ell. \tag{6}$$

THEOREM 2.1   *Assume that the input sequence $\{u_k\}$ on $\mathbb{R}$ is bounded. Then the stochastic nonlinear system (5) is second moment stable if all the eigenvalues of the matrix*

$$\mathcal{A} \otimes \mathcal{A} + \sum_{i=1}^{\ell} \mathcal{H}_i \otimes \mathcal{H}_i$$

lie inside the unit circle.

Remark 2   The result of Theorem 2.1 allows us to check whether a nonlinear stochastic system as in (5) is second moment stable through a simple numerical evaluation. The result can then be used to check whether an identification procedure is successful on generating a stable model. This property is illustrated in this paper for a real-time automotive engine, as described in Section 3.

2.1. Proof of Theorem 2.1

Proof   Before presenting the main argument for the proof of Theorem 2.1, we need some preliminary results. Consider the identify

$$[A_{[1]}, \dots, A_{[2(d+1)+1]}] Y_k = \sum_{n=0}^{d} A_{[n+1]} y_{k-n} + \left\{ \sum_{n=0}^{d} A_{[n+d+2]} u_{k-n} \right\}. \tag{7}$$

cogent · engineering

Similarly, for each $i = 1, \ldots, \ell$, we can write

$$W_{[i],k}\left[H_{[1],i}, \ldots, H_{[2(d+1)+1],i}\right]Y_k = W_{[i],k}\sum_{n=0}^{d}H_{[n+1],i}y_{k-n} + \left\{W_{[i],k}\left(\sum_{n=0}^{d}H_{[n+d+2],i}u_{k-n}\right)\right\}. \tag{8}$$

Summing up for i the elements inside the rightmost curly brackets of (8), and adding in this evaluation the term the rightmost curly brackets of (7), we obtain a random value, say $\varphi(Y_k, W_k)$. We have immediately from (5) that

$$y_{k+1} = \sum_{n=0}^{d}\left(A_{[n+1]} + \sum_{i=1}^{\ell}W_{[i],k}H_{[n+1],i}\right)y_{k-n} + \varphi(Y_k, W_k) + g(Y_k), \quad \forall k \geq s. \tag{9}$$

Applying in (9) the matrices $\mathcal{A}, \mathcal{H}_i, i = 1, \ldots, \ell$, as defined in (6), we obtain the next identity:

$$\begin{bmatrix} y_{k-d+1} \\ \vdots \\ y_{k+1} \end{bmatrix} = \left(\mathcal{A} + \sum_{i=1}^{\ell}W_{[i],k}\mathcal{H}_i\right)\begin{bmatrix} y_{k-d} \\ \vdots \\ y_k \end{bmatrix} + \left(\varphi(Y_k, W_k) + g(Y_k)\right)\begin{bmatrix} 0 \\ \vdots \\ 0 \\ 1 \end{bmatrix}. \tag{10}$$

Notice that (5) and (10) are equivalent. Now, for sake of notational simplicity, let us fix

$$z_k \equiv [y_{k-d}, \ldots, y_k], \quad \mathcal{F}_k \equiv \mathcal{A} + \sum_{i=1}^{\ell}W_{[i],k}\mathcal{H}_i, \quad \mathcal{B}_k \equiv \left(\varphi(Y_k, W_k) + g(Y_k)\right)\begin{bmatrix} 0 \\ \vdots \\ 0 \\ 1 \end{bmatrix}.$$

With this notation, (10) is identical to $z_{k+1} = \mathcal{F}_k z_k + \mathcal{B}_k$, which in turn is identical to

$$z_{k+1} = \mathcal{F}_k \cdots \mathcal{F}_s z_s + \sum_{j=s}^{k}\mathcal{F}_k \cdots \mathcal{F}_{j+1}\mathcal{B}_j, \quad \forall k \geq s, \quad \forall s > d. \tag{11}$$

Let us now introduce a result, necessary here to continue with the argument.

LEMMA 2.1   *The eigenvalues of the matrix $\mathcal{A} \otimes \mathcal{A} + \sum_{i=1}^{\ell}\mathcal{H}_i \otimes \mathcal{H}_i$ lie inside the unit circle if and only if there exists two constants $\beta \geq 1$ and $0 < \alpha < 1$ such that*

$$\mathsf{E}\left[\|\mathcal{F}_k \cdots \mathcal{F}_s\|^2\right] \leq \beta\alpha^{k-s}, \quad \forall k \geq s.$$

The proof of Lemma 2.1 is available in Appendix 1. The proof of the next result follows from the fact that $\sup_{x \in \mathbb{R}^s} g(x)$ is a finite value (see Remark 1).

LEMMA 2.2   *There exists a constant $c > 0$ such that $\mathsf{E}\left[\|\mathcal{B}_k\|^2\right] \leq c$ for all $k > d$.*

Now we present the last argument to prove Theorem 2.1. For this purpose, we show that the sequence $\{\mathsf{E}[\|z_k\|^2]\}$ is uniformly bounded–with z_k as in (11); this assures that the stochastic nonlinear system (5) is second moment stable according to Definition 1.1.

Applying the Euclidean norm on both sides of (11), and passing the expected value operator, we have

$$\mathsf{E}\left[\|z_{k+1}\|^2\right] \leq \mathsf{E}\left[\|\mathcal{F}_k \cdots \mathcal{F}_s z_s\|^2\right] + \sum_{j=s}^{k}\mathsf{E}\left[\|\mathcal{F}_k \cdots \mathcal{F}_{j+1}\mathcal{B}_j\|^2\right], \quad \forall k \geq s. \tag{12}$$

Finally, Lemmas 2.1 and 2.2 used in (12) assure that $E\left[\|z_{k+1}\|^2\right]$ is bounded above by $\beta\alpha^{k-s} E[\|z_s\|^2] + \alpha^{-s}c/(1-\alpha)$ for all $k \geq s$. Since s was taken arbitrarily in (11), one can set $s = 0$ and the result follows. □

3. Model for the intake manifold pressure: experimental approach

The laboratory testbed used in the experiments was equipped with an automotive engine mock-up, Model Volkswagen AT EA-111 RSH 1.0 Total Flex, with four cylinders and eight valves, used in the cars manufactured by Volkswagen models VW Gol and VW Fox (see Figure 2). This engine can be fueled with gasoline or ethanol, or if needed with any mixture of them, but the experiments were carried out with ethanol only.

In our experiments, we were interested in finding a single-input single-output model to characterize the relation between the throttle valve (input) and pressure MAP sensor (output). To obtain measurements for both input and output, we used a data acquisition card model NI-USB 6008 to measure the voltages informed by the two corresponding sensors. The engine has built-in sensors for both variables, that is, the pressure is measured by the MAP sensor (Figure 1) and the angle of aperture of the throttle is measured by its corresponding sensor assembled in the valve plate. The sampling time of the data acquisition card was kept fixed at 5 milliseconds. For this investigation, the engine was operated at no load condition.

By pressing manually the gas pedal, we generated a movement in the angle of the throttle valve and this induced a dynamics for the intake manifold pressure, see Figure 3 for a pictorial representation. Part of this experimental data was selected to identify the model as in (5) whereas the remaining data was used for model validation. In this study, we used a least square routine with no noise input in the model in (5) (i.e. $W_k \equiv 0$).

The values of the identified parameters of (5) are omitted here for sake of brevity, but for an account we mention that $d = 5$ in (1) (quantity of regressors) and $n = 8$ in (3).

The identified model as in (5) with no noise input presented a fit value of 67% when compared with real data. However, although the combustion engine is a highly complex system, the fit of 67% is a positive indication that confirms the difficulty on characterizing precisely the throttle-MAP relation; such lack of precision is recurrent in the literature (Alberer, Hirsch, & del Re, 2010; Ortner & del Re, 2007; Wahlström & Eriksson, 2011).

**Figure 2. Picture of the engine mock-up used in the experiments.**
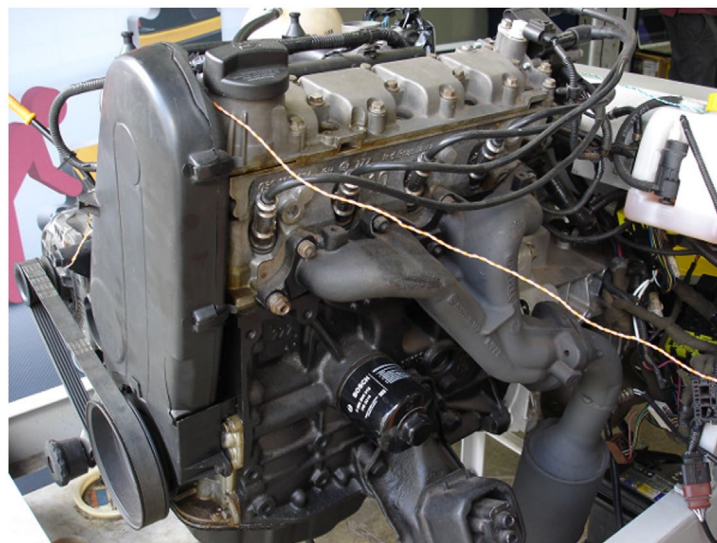
Figure 3. Experimental data: sample rate at 5 ms. Notes: Upper: angle of the throttle valve (input). Lower: intake manifold pressure (output)–the real-time measured data is in the black curve; and simulated data via the model in (5) with no noise input (i.e., $W_k \equiv 0$) is in the red curve. The simulated and experimental curves presented a fit of 67%.
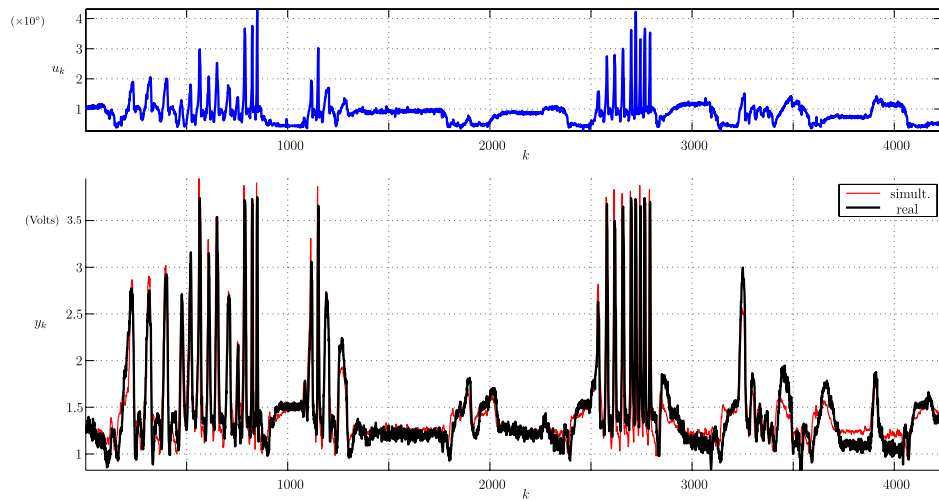
Figure 4. Comparison of the data obtained from a Monte-Carlo simulation with the one taken from an experiment made in the mock-up. The central curve in black represents the mean of the Monte-Carlo simulation whereas the red shading around it delimits the standard deviation. The experimental data in dotted blue lies within the region of feasibility of the stochastic model.
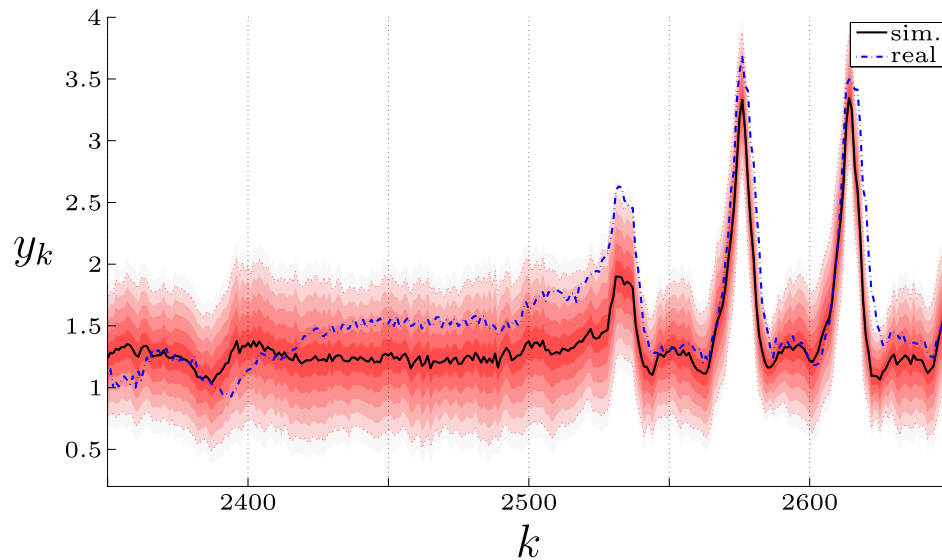
Figure 5. Localization of eigenvalues in the complex plane. The data corresponds to the model of an automotive throttle-MAP relation. All of the eigenvalues are inside the unit disc, which shows that the automotive model is second moment stable.
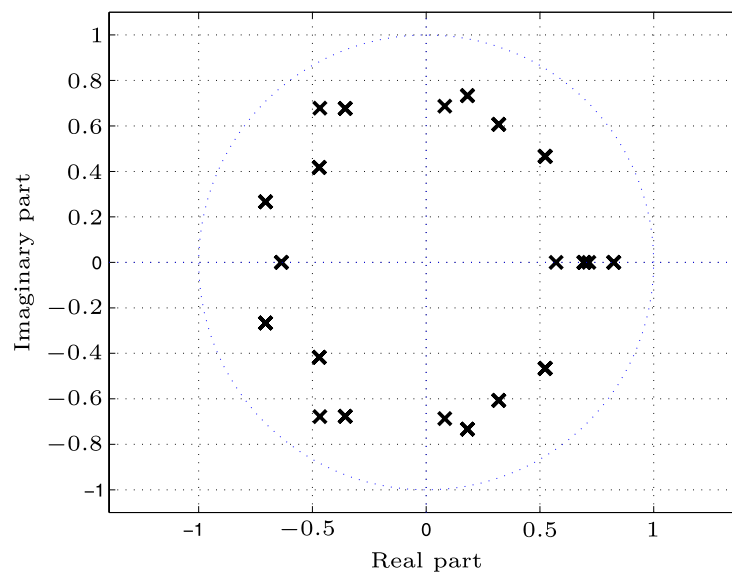
As an attempt to improve the throttle-MAP relation, we assumed that $\{W_k\}$ in (5) is a standard Gaussian white noise processes. And to illustrate the influence of such noise in the proposed throttle-MAP model, we generated a Monte-Carlo simulation with eight hundred realizations. Interestingly, the real data lies within the feasible region covered by the simulated data, as can be seen in Figure 4. This evidence suggests that (5) can be a candidate for representing the throttle-MAP dynamics.

Finally, a question of practical interest is to determine whether the identified throttle-MAP model as in (5) is second moment stable. The identified parameters to be checked are (recall that $d = 5$)

$$\begin{bmatrix} A_{[d+1]} \\ A_{[d]} \\ \vdots \\ A_{[1]} \end{bmatrix} = \begin{bmatrix} 0.3625 \\ -0.2305 \\ -0.3124 \\ 0.2265 \\ 0.1362 \\ 0.4872 \end{bmatrix}$$

and each value in $H_{[j],i}$, $j = 1, \ldots, 13$, $i = 1, \ldots, 6$, assumes 0.05 when $i = j$ and zero elsewhere. Using these values to generate the matrix $\mathcal{A} \otimes \mathcal{A} + \sum_{i=1}^{\ell} \mathcal{H}_i \otimes \mathcal{H}_i$ (e.g. (6)), we can conclude that its eigenvalues are located inside the unit disc (Figure 5). Hence, Theorem 2.1 guarantees that the identified throttle-MAP model is second moment stable. This illustrates the practical usefulness of Theorem 2.1.

4. Concluding remarks

We have presented a simple numerical condition to check the second moment stability of single-input single-output stochastic nonlinear systems. Such a stochastic system can be accounted to represent the throttle-MAP dynamics of a spark-ignition engine fueled with ethanol.

Data taken from real-time experiments suggest that throttle-MAP process is second moment stable, an evidence that corroborates the theoretical result.

As further investigation goes on, control of the MAP can be a useful for vehicle platooning (Liang, Måartensson, Johansson, 2016).

Author details
Alessandro N. Vargas[1]
E-mail: avargas@utfpr.edu.br
Leonardo Acho[2]
E-mail: leonardo.acho@upc.edu
Edison Bonifacio[3]
E-mail: edison.bonifacio@pr.senai.br
Walter Arens[4]
E-mail: Walter.Arens@br.bosch.com
João B.R. do Val[4]
E-mail: jbosco@fee.unicamp.br
[1] Universidade Tecnológica Federal do Paraná, UTFPR, Av. Alberto Carazzai 1640, 86300-000 Cornelio, Procópio-PR, Brazil.
[2] CoDAlab (Control, Dynamics and Applications), Departament de Matemàtica Aplicada III, Universitat Politècnica de Catalunya, Comte d'Urgell, 187, 08036 Barcelona, Spain.
[3] Serviço Nacional de Aprendizagem Industrial, SENAI, Rua Belem, 844, 86026-000 Londrina-PR, Brazil.
[4] Universidade Estadual de Campinas, UNICAMP, FEEC, Av. Albert Einstein 400, 13083-852 Campinas-SP, Brazil.

References
Alberer, D., Hirsch, M., & del Re, L. (2010). A virtual references design approach for diesel engine control optimization. *Control Engineering Practice, 18*, 1263–1271.
Arnold, L. (1974). *Stochastic differential equations: Theory and applications*. Hoboken, NJ: Wiley-Interscience.
Balluchi, A., Benvenuti, L., Di Benedetto, M. D., Pinello, C., & Sangiovanni-Vincentelli, A. L. (2000). Automotive engine control and hybrid systems: challenges and opportunities. *Proceedings of the IEEE, 88*, 888–912.

Brewer, J. W. (1978). Kronecker products and matrix calculus in system theory. *IEEE Transactions on Circuits and Systems, 25*, 772–781.

Casavola, A., Famularo, D., & Gagliardi, G. (2013). A linear parameter varying fault detection and isolation method for internal combustion spark ignition engines. *International Journal of Robust and Nonlinear Control.* doi:10.1002/rnc.3128

Fleming, W. J. (2001). Overview of automotive sensors. *IEEE Sensors Journal, 1*, 296–308.

Guzzella, L., & Onder, C. (2010). *Introduction to Modeling and Control of Internal Combustion Engine Systems* (2nd ed.). New York, NY: Springer.

Hendricks, E. (1997). Engine modelling for control applications: A critical survey. *Meccanica, 32*, 387–396.

Hendricks, E., & Sorenson, S. (1990). Mean value modelling of spark ignition engines. *SAE Transactions, 99*, 1359–1373.

Heywood, J. (1988). Internal Combustion Engine Fundamentals. *Series in Mechanical Engineering.* New York, NY: McGraw-Hill Publishing.

Kubrusly, C. S., & Costa, O. (1985). Mean square stability conditions for discrete stochastic bilinear systems. *IEEE Transactions on Automatic Control, 30*(11), 1082–1087.

Liang, K. Y., M{\aa}rtensson, J. & Johansson, K. H. (2016). Heavy-duty vehicle platoon formation for fuel efficiency. *IEEE Transactions on Intelligent Transportation Systems, 17*, 1051–1061.

Li, Y., Sui, S., & Tong, S. (2016). Adaptive fuzzy control design for stochastic nonlinear switched systems with arbitrary switchings and unmodeled dynamics. *IEEE Transactions on Cybernetics, 99*, 1–2.

Ljung, L. (Ed.). (1999). *System identification: Theory for the user* (2nd ed.). Upper Saddle River, NJ: Prentice Hall.

Ortner, P., & del Re, L. (2007). Predictive control of a diesel engine air path. *IEEE Transactions on Control Systems Technology, 15*, 449–456.

Pearson, R. K. (2003). Selecting nonlinear model structures for computer control. *Journal of Process Control, 13*(1), 1–26.

Sjöberg, J., Zhang, Q., Ljung, L., Benveniste, A., Delyon, B., Glorennec, P.-Y., … Juditsky, A. (1995). Nonlinear black-box modeling in system identification: A unified overview. *Automatica, 31*, 1691–1724.

Stotsky, A. A. (2009). *Automotive Engines: Control, Estimation, Statistical Detection*. New York, NY: Springer.

Tang, H., Weng, L., Dong, Z., & Yan, R. (2009). Adaptive and learning control for SI engine model with uncertainties. *IEEE/ASME Transactions on Mechatronics, 14*, 93–104.

Vargas, A. N., & do Val, J. B. R. (2010). Average cost and stability of time-varying linear systems. *IEEE Transactions on Automatic Control, 55*, 714–720.

Wahlström, J., & Eriksson, L. (2011). Modelling diesel engines with a variable-geometry turbocharger and exhaust gas recirculation by optimization of model parameters for capturing non-linear system dynamics. *Proceedings of the Institution of Mechanical Engineers, Part D: Journal of Automobile Engineering, 225*, 960–986.

Wu, Z., Cui, M., Shi, P., & Karimi, H. R. (2013). Stability of stochastic nonlinear systems with state-dependent switching. *IEEE Trans. Automat. Control, 58*, 1904–1918.

Yin, J., Khoo, S., Man, Z., & Yu, X. (2011). Finite-time stability and instability of stochastic nonlinear systems. *Automatica, 47*, 2671–2677.

Zhao, P., Feng, W., & Kang, Y. (2012). Stochastic input-to-state stability of switched stochastic nonlinear systems. *Automatica, 48*, 2569–2576.

Appendix 1

Appendix–Proof of Lemma 2.1

Proof The proof of Lemma 2.1 is inspired in the arguments used in Kubrusly and Costa (1985, Proposition 6). To begin with, we have from the i.i.d. assumption on $\{W_k\}$ that

$$\mathsf{E}\left[W_{[i],k}\mathcal{H}_i \otimes W_{[j],k}\mathcal{H}_j\right] = 0, \quad i \neq j, \quad \text{and} \quad \mathsf{E}\left[W_{[i],k}\mathcal{H}_i \otimes W_{[i],k}\mathcal{H}_i\right] = \mathcal{H}_i \otimes \mathcal{H}_i,$$

which allow us to write

$$\mathcal{A} \otimes \mathcal{A} + \sum_{i=1}^{\ell} \mathcal{H}_i \otimes \mathcal{H}_i = \mathsf{E}\left[\left(\mathcal{A} + \sum_{i=1}^{\ell} W_{[i],k}\mathcal{H}_i\right) \otimes \left(\mathcal{A} + \sum_{i=1}^{\ell} W_{[i],k}\mathcal{H}_i\right)\right], \quad \forall k \geq s. \tag{13}$$

On the other hand, by defining the autonomous linear stochastic recurrence

$$q_{k+1} = \left(\mathcal{A} + \sum_{i=1}^{\ell} W_{[i],k}\mathcal{H}_i\right)q_k, \quad \forall k \geq s, \quad q_s \in \mathbb{R}^n,$$

one can evaluate the second moment matrix $Q_k \equiv \mathsf{E}[q_k q_k']$ as follows:

$$Q_{k+1} = \mathsf{E}\left[\left(\mathcal{A} + \sum_{i=1}^{\ell} W_{[i],k}\mathcal{H}_i\right)q_k q_k'\left(\mathcal{A} + \sum_{i=1}^{\ell} W_{[i],k}\mathcal{H}_i\right)'\right]. \tag{14}$$

cogent engineering

Applying the stacking operator $\mathsf{vec}(\cdot)$ on both sides of (14), and considering the identity in (13), we have

$$\mathsf{vec}(Q_{k+1}) = \mathsf{E}\left[\left(\mathcal{A} + \sum_{i=1}^{\ell} W_{[i],k}\mathcal{H}_i\right) \otimes \left(\mathcal{A} + \sum_{i=1}^{\ell} W_{[i],k}\mathcal{H}_i\right)\right] \mathsf{vec}(Q_k)$$

$$= \left(\mathcal{A} \otimes \mathcal{A} + \sum_{i=1}^{\ell} \mathcal{H}_i \otimes \mathcal{H}_i\right) \mathsf{vec}(Q_k). \tag{15}$$

Since (15) is a linear deterministic autonomous system, we can conclude that $\mathsf{vec}(Q_k) \to 0$ as $k \to \infty$ if and only if the eigenvalues of $\mathcal{A} \otimes \mathcal{A} + \sum_{i=1}^{\ell} \mathcal{H}_i \otimes \mathcal{H}_i$ lie within the unit circle. This is equivalent to observe the exponential decay of Q_k when k increases, or equivalently, to the existence of two constants $\beta \geq 1$ and $0 < \alpha < 1$ such that

$$\mathsf{E}\left[\|q_k\|^2\right] = \mathsf{E}[\, \mathsf{tr}\{q_k q_k'\}] = \mathsf{tr}\{\,\mathsf{E}[q_k q_k']\} = \mathsf{tr}\{Q_k\} \leq \beta\alpha^{k-s}.$$

This argument completes the proof of Lemma 2.1. $\qquad\qquad\square$

Cogent Engineering (ISSN: 2331-1916) is published by Cogent OA, part of Taylor & Francis Group.

Publishing with Cogent OA ensures:

- Immediate, universal access to your article on publication
- High visibility and discoverability via the Cogent OA website as well as Taylor & Francis Online
- Download and citation statistics for your article
- Rapid online publication
- Input from, and dialog with, expert editors and editorial boards
- Retention of full copyright of your article
- Guaranteed legacy preservation of your article
- Discounts and waivers for authors in developing regions

Submit your manuscript to a Cogent OA journal at www.CogentOA.com